Numerical estimation of carbonate properties using a digital rock physics workflow

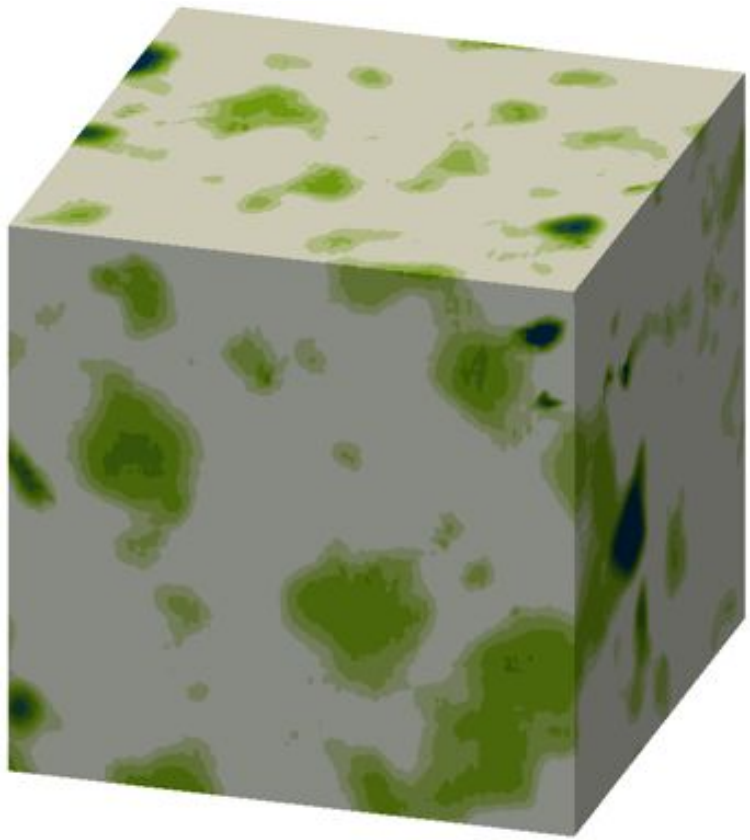

Maria Osorno[2]
David Uribe[1]
Erik H. Saenger[3]
Claudio Madonna[3]
Holger Steeb[1]
Oscar Ruiz[2]

[1] Institute of Mechanics, Ruhr-University Bochum
[2] CAD/CAM/CAE Laboratory, Universidad EAFIT
[3] Geological Institute, ETH Zürich

EAGE 17.06.2014

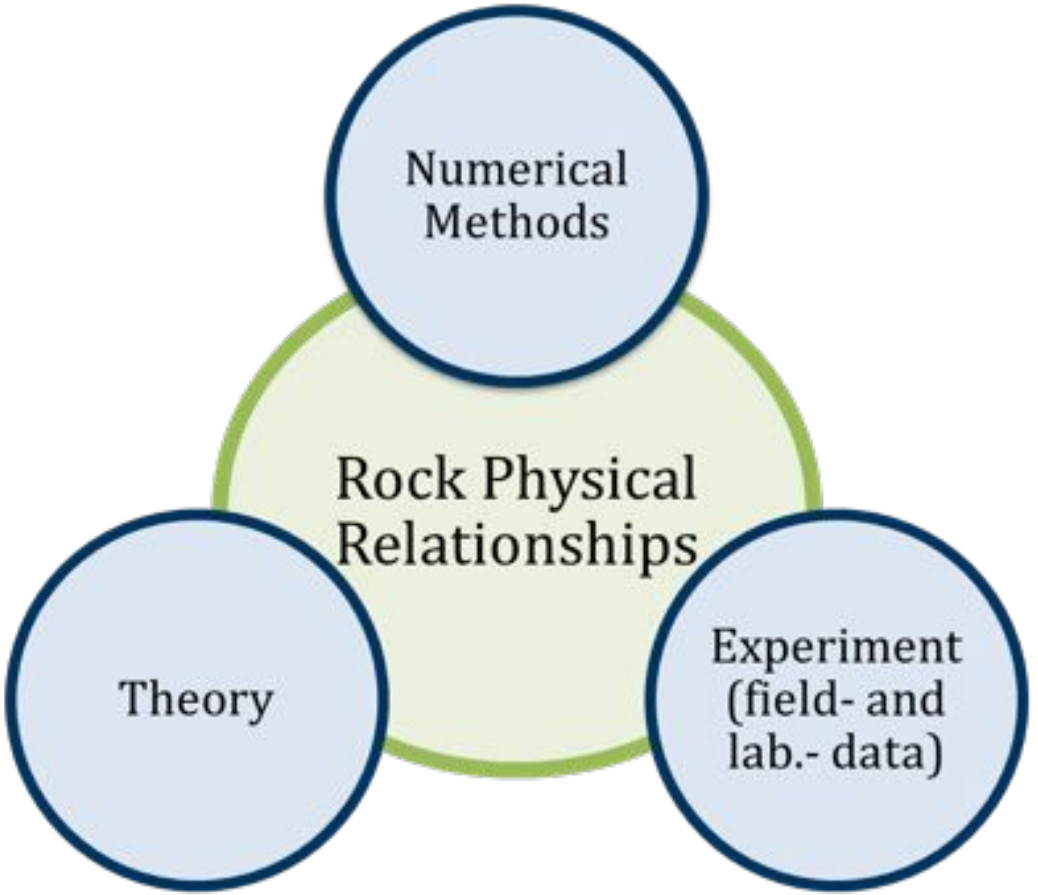

Macro-, Meso- and Microscale

Motivation

1. Estimate effective material parameters of porous materials from micro Computer Tomography (μCT) digital samples.
2. Overcome the resolution/sample-size problem inherent of μCT based methods.
3. Analyse how the image segmentation affects the estimation of effective material parameters of porous materials.

Scale-dependent digital images

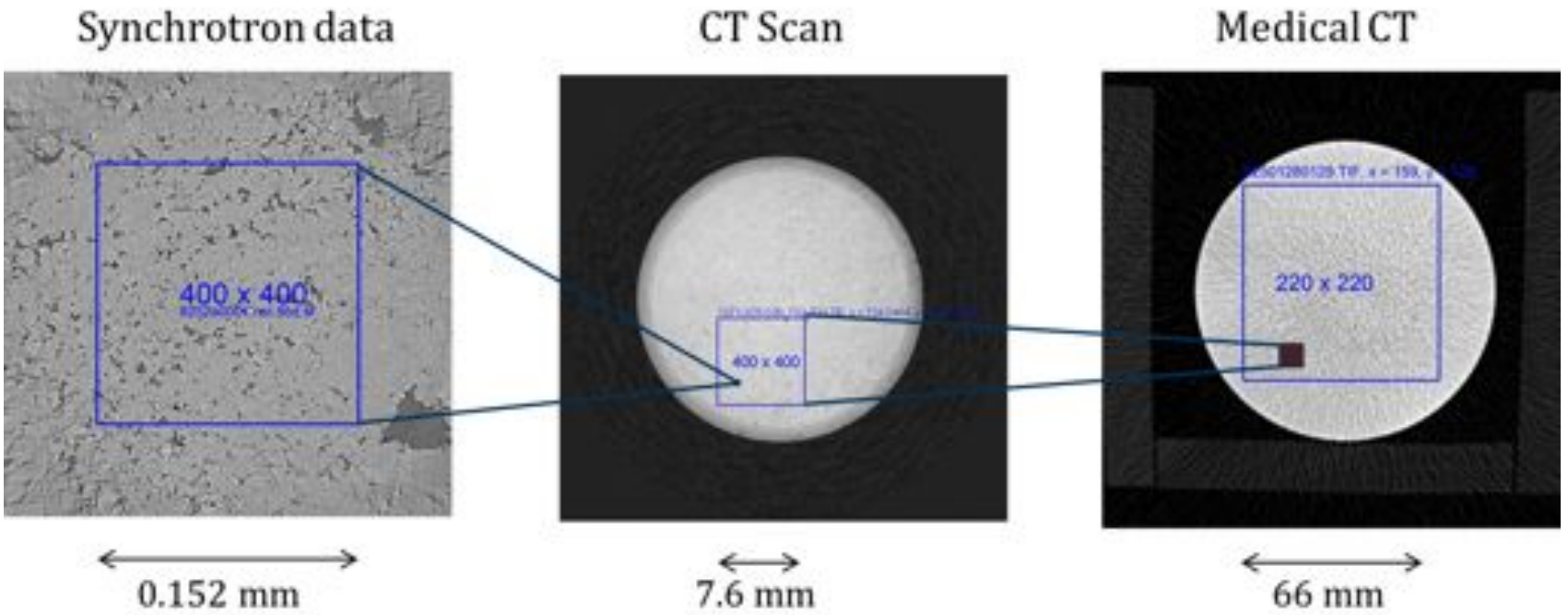

$dx = 0.38\ \mu$m
$\phi_{\text{image}} = 0.12$
$Vp(\text{num}) = 5699$ m/s
$Vs(\text{num}) = 3560$ m/s

$dx = 19\ \mu$m
$\phi_{\text{image}} = 0.0025$
$Vp(\text{num}) = 5690$ m/s
$Vs(\text{num}) = 3550$ m/s

$dx = 300\ \mu$m
$\phi_{\text{image}} = 0.014$
$Vp(\text{num}) = 5535$ m/s
$Vs(\text{num}) = 3482$ m/s

Porosity determination from raw digital images

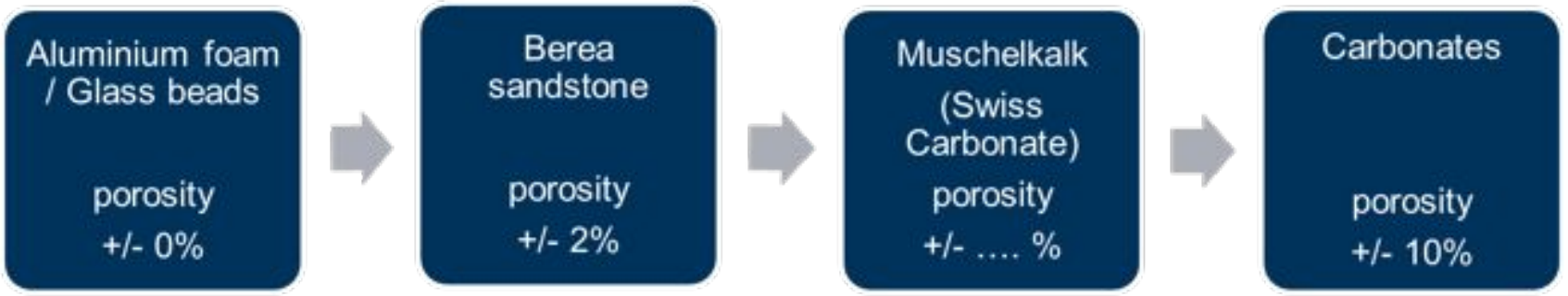

Permeability

(lower bound estimate for representative ensemble)

...vice-versa strategy to effective elastic properties.
(in addition to connected vs. total porosity)

Analysed Sample

Dry carbonate specimen (Hauptmuschelkalk) from a core drilled in northern Switzerland[1]

[1] CT-image raw-data from Madonna C. et al. [2013] Synchrotron-based X-ray tomographic microscopy for rock microstructure investigations. Geophysics, 78, D53-D64.

Image Segmentation

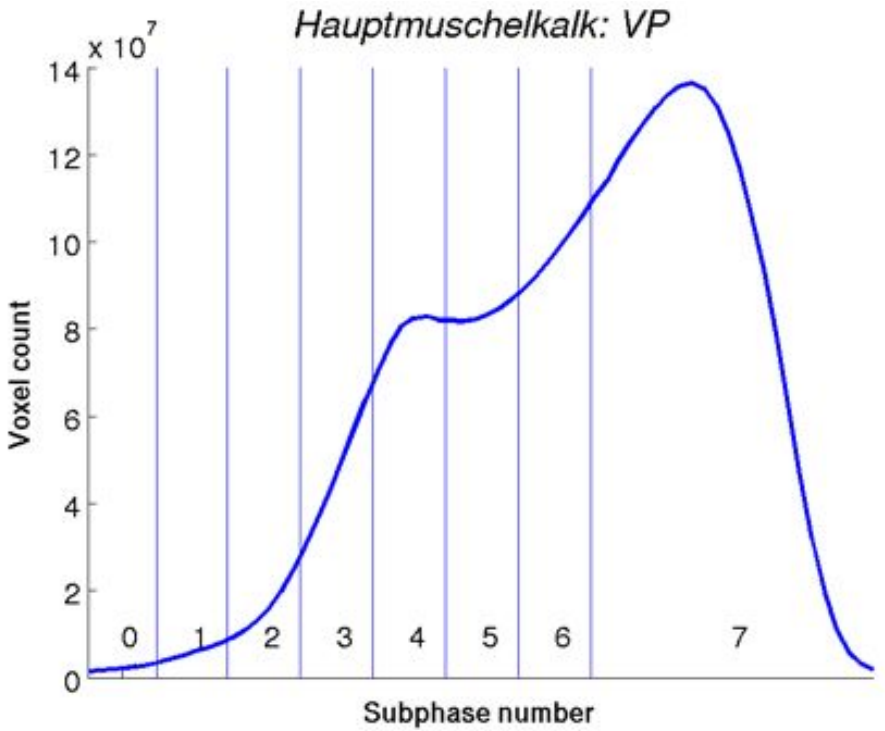

X-Ray absorption vs. Count size after applying a 3D non-local mean filter

The Carbonate segmentation problem

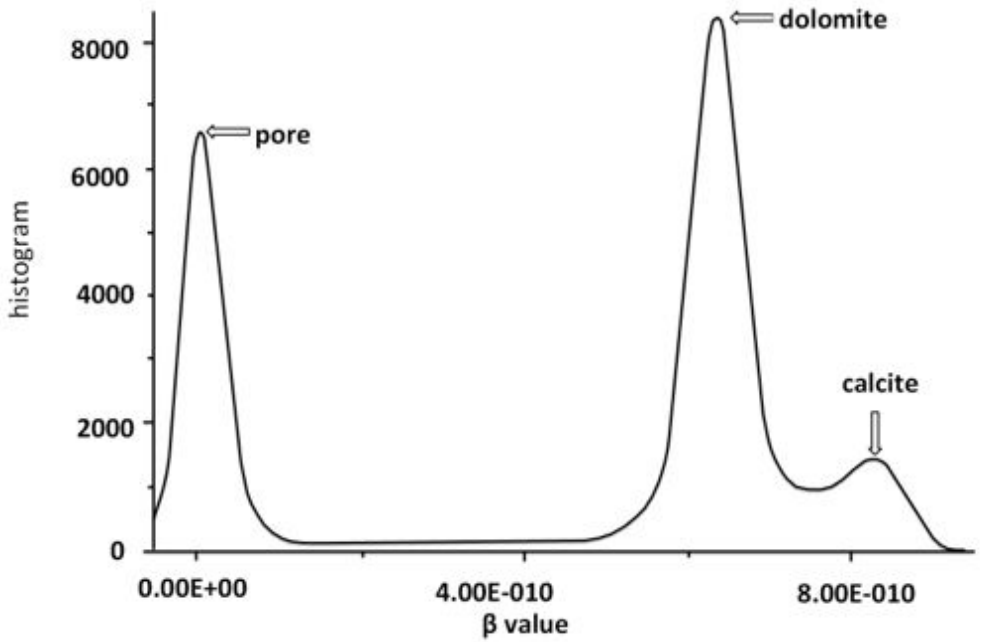

Wang, Y., Y. Yang, T. Xiao, K. Liu, B. Clennell, G. Zhang, H. Wang, 2013, Synchrotron-Based Data-Constrained Modeling Analysis of Microscopic Mineral Distributions in Limestone: International Journal of Geosciences, 4, 344-351, http://dx.doi.org/10.4236/ijg.2013.42032.

Two phases

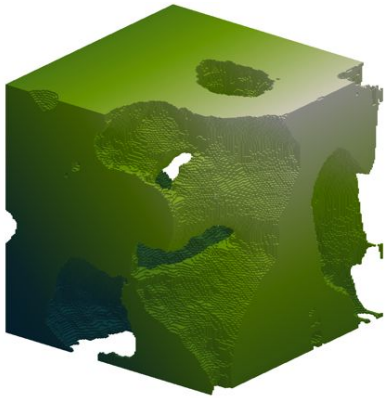

$T = 7$

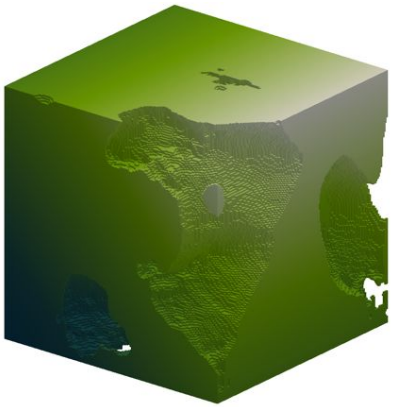

$T = 6$

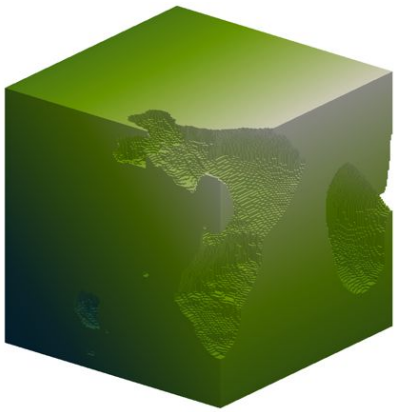

$T = 5$

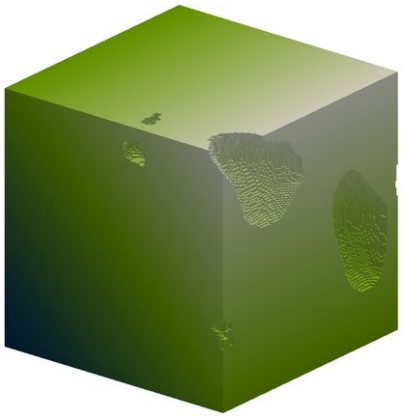

$T = 4$

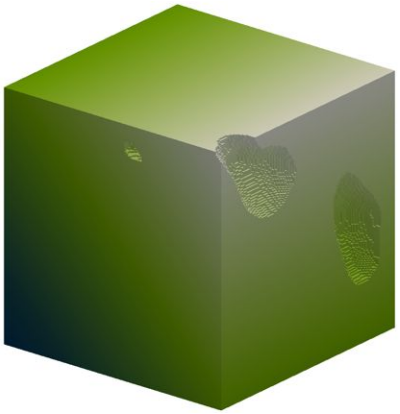

$T = 3$

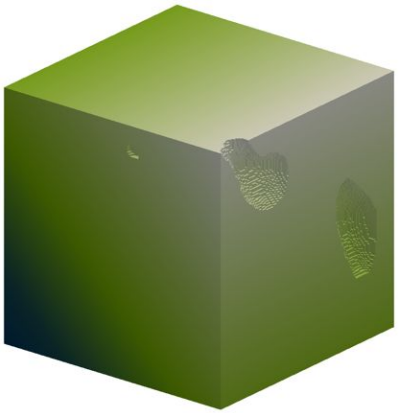

$T = 2$

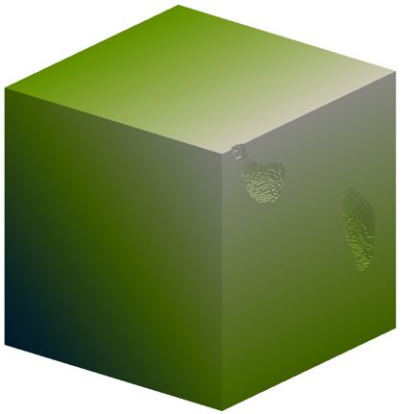

$T = 1$

Subdomains of solid phase after threshold.

Elastic Moduli

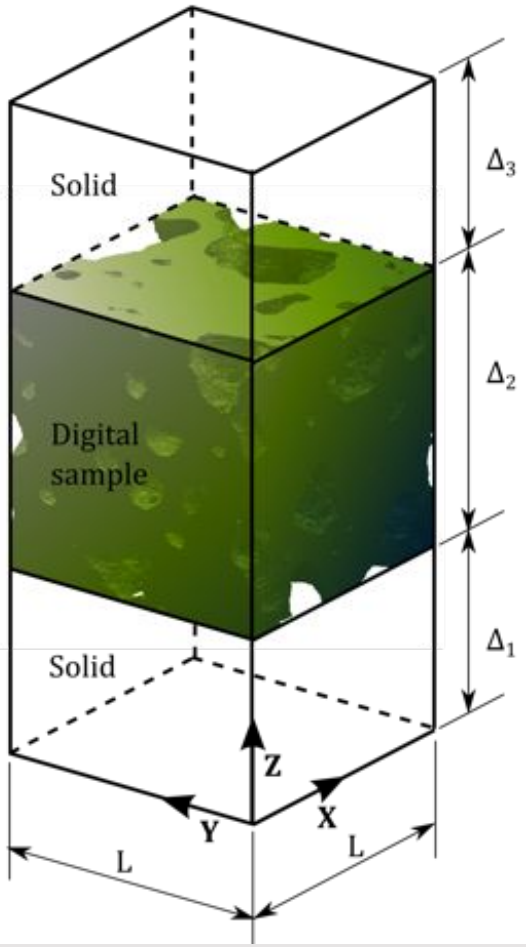

Elastic Moduli

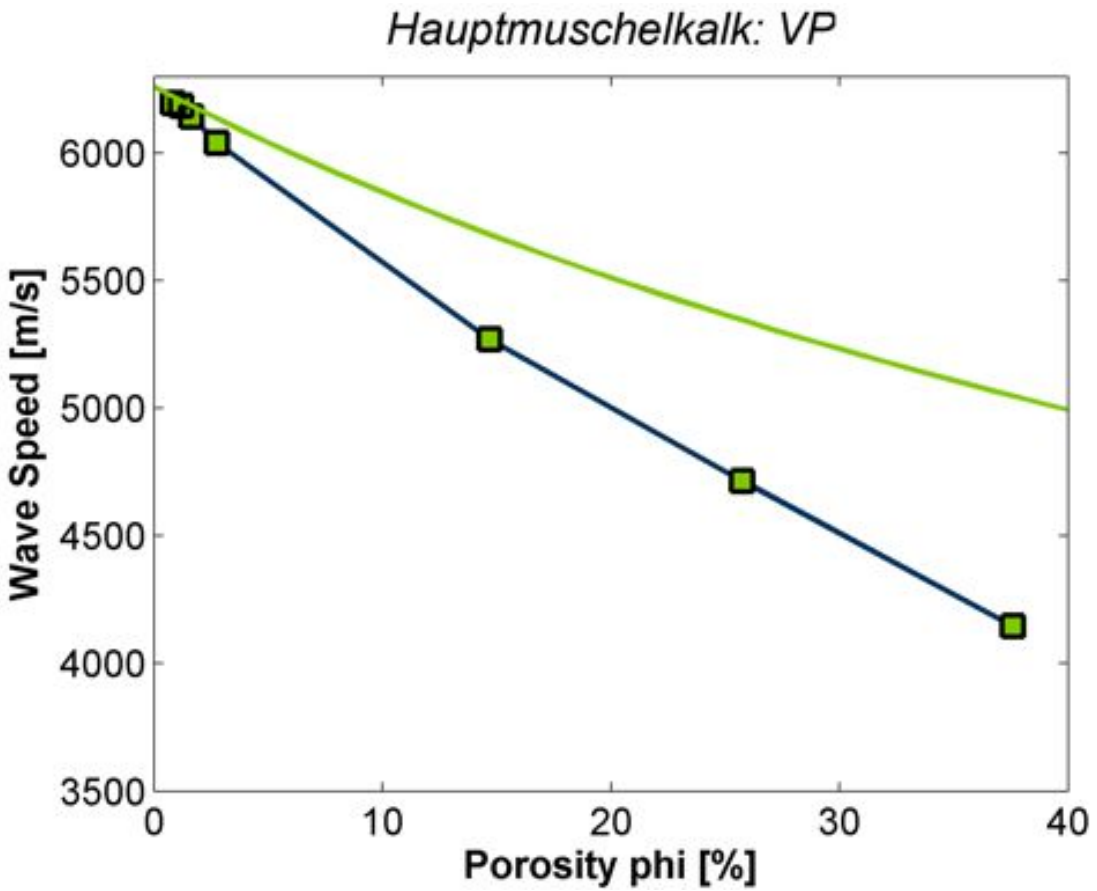

— Upper HS bound

■ Simulations with two phases

Permeability

Permeability

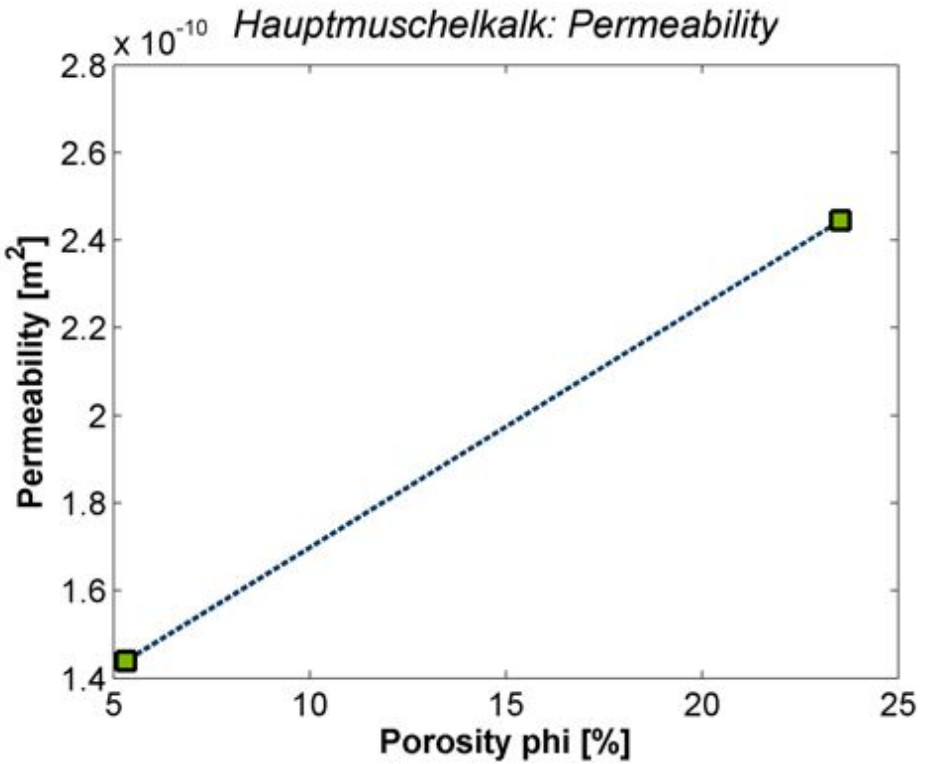

- Simulations with two phases

Permeability with respect to the connected porosity.

With porosities below 5% the geometry does not present connected pores, and permeability is estimated to be 0 mD.

Three phases

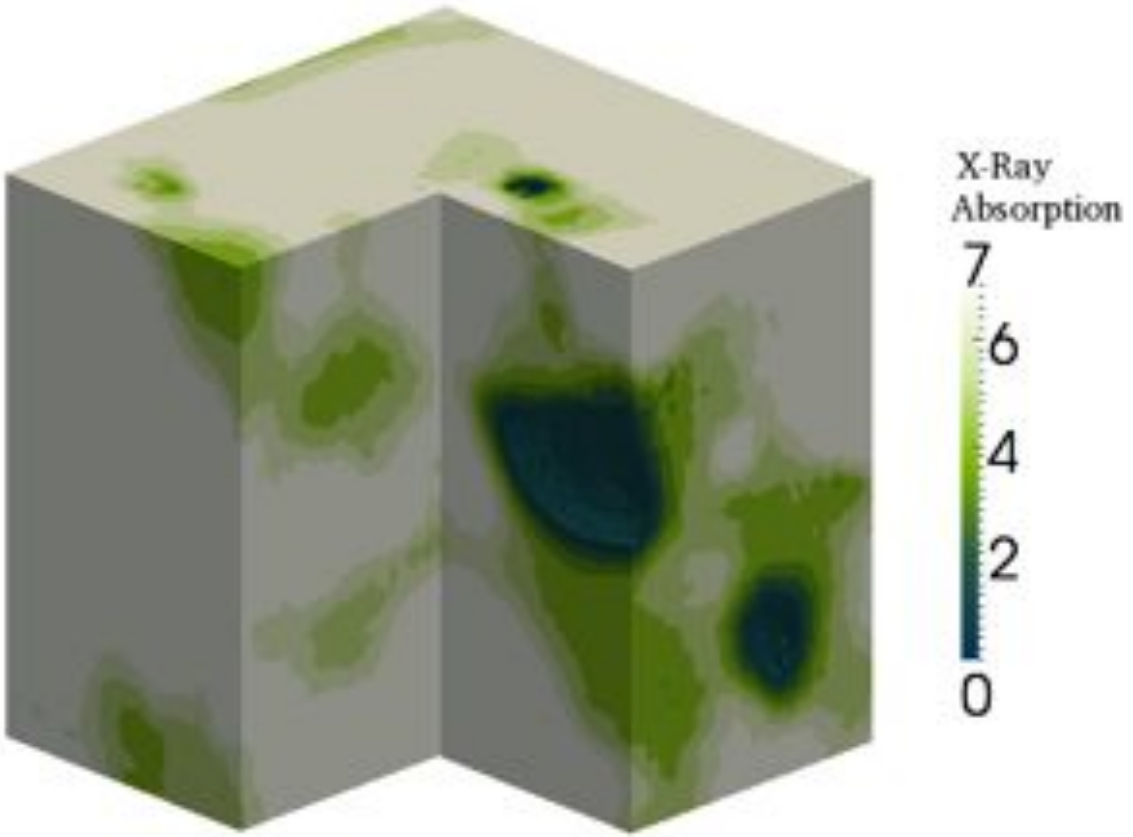

Elastic Moduli

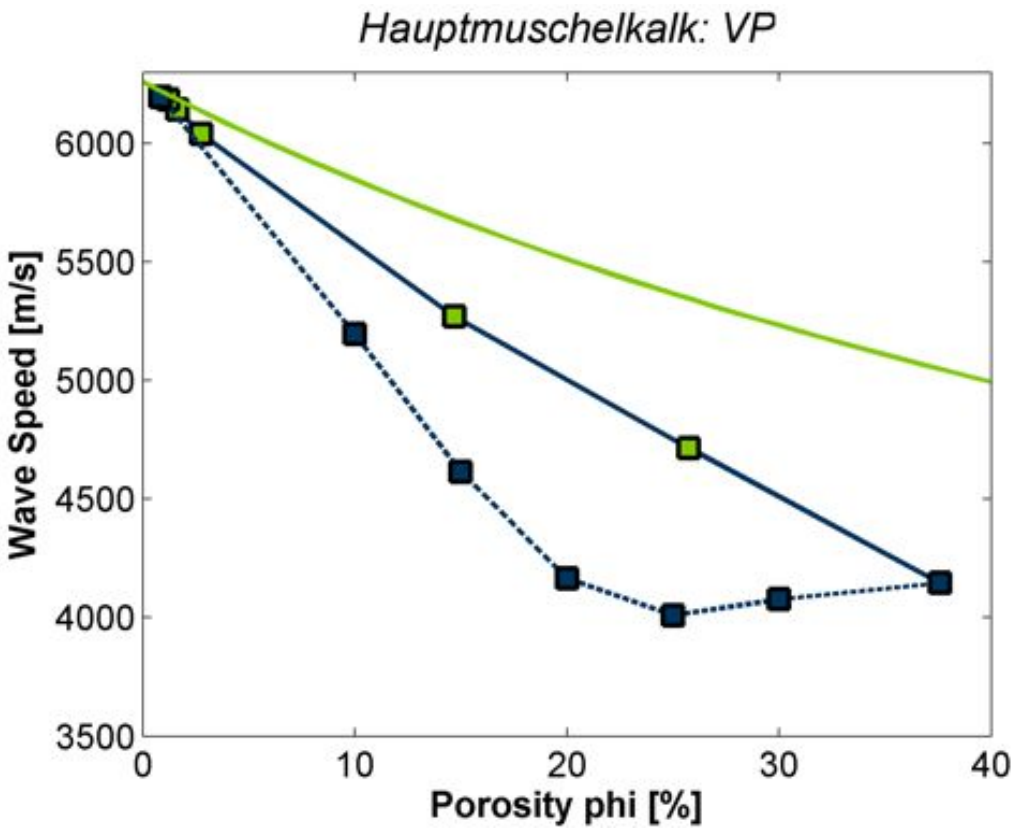

- Upper HS bound
- Simulations with two phases
- Simulations with three phases
- Observed Vp trend

Elastic Moduli

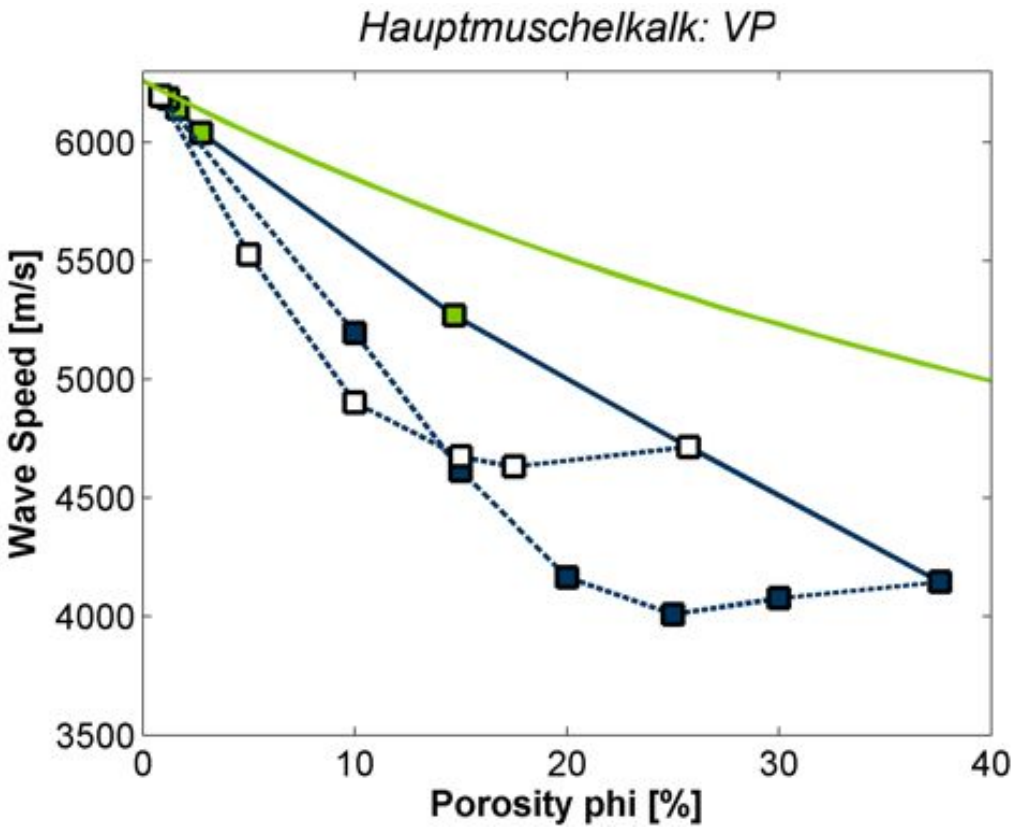

- Upper HS bound
- Simulations with two phases
- Simulations with three phases
- Simulations with three phases
- Observed Vp trend

Experimental results

Porosity	4,2%
Permeability	4×10^{-4} mD
P-Wave velocity (0 MPa confining pressure)	5100 m/s
P-Wave velocity (150 MPa confining pressure)	6100 m/s

R. Shih, 2012, Simulating the in situ physical properties of the upper Muschelkalk aquifer. Master thesis, ETH Zurich.

Elastic Moduli - Experimental Results

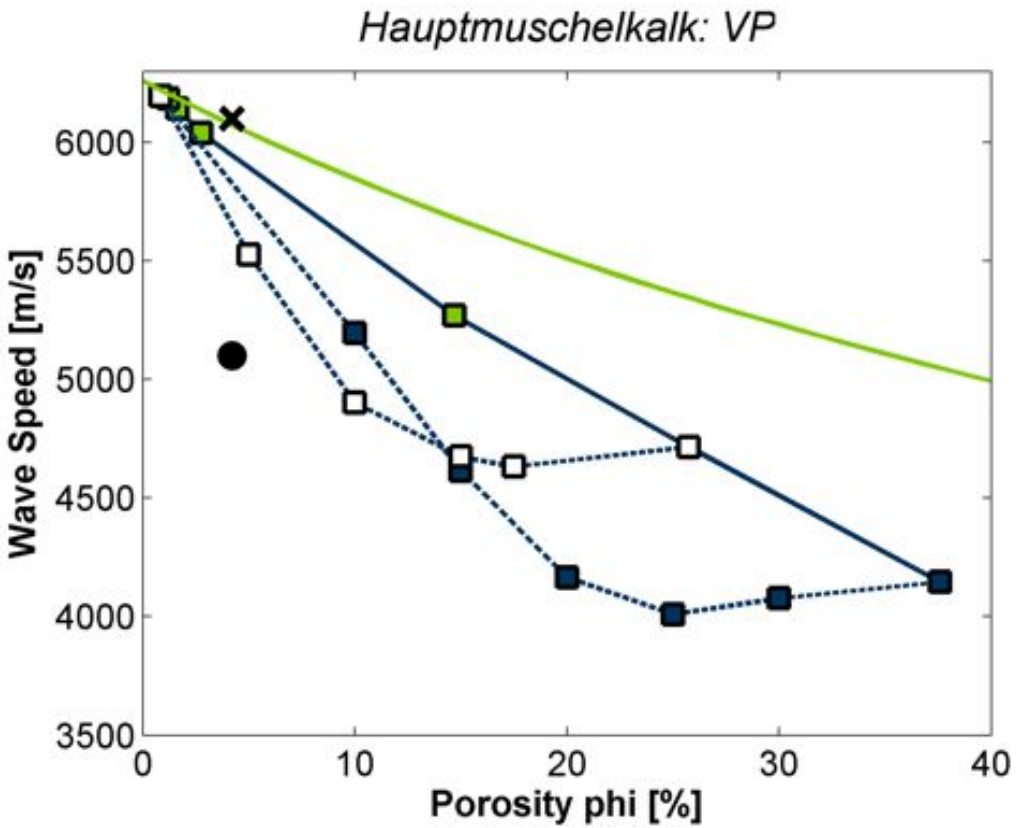

- Upper HS bound
- Simulations with two phases
- Simulations with three phases
- Simulations with three phases
- Observed Vp trend
- Experimental result (0 Mpa confining pressure)
- Experimental result (150 Mpa confining pressure)

Conclusions